Pieroni, L., Elettore, E., Freddi, F., Latour, M. (2021) Optimized strategies for mid-rise seismic-resilient self-centring steel moment resisting frames. The 9th European Conference on Steel and Composite Structures (Eurosteel 2020), Sheffield, UK, 1–3 September 2021. https://doi.org/10.1002/cepa.1521

Optimised Strategies for Seismic-Resilient Self-Centring Steel Moment Resisting Frames

Ludovica Pieroni[1], Elena Elettore[2], Fabio Freddi[1], Massimo Latour[2]

Correspondence

Ludovica Pieroni
PhD Student
University College London
Department of Civil, Environmental and Geomatic Engineering

Chadwick Building, Gower Street
WC1E 6BT London
Email: ludovica.pieroni.20@ucl.ac.uk

Abstract

In recent years there have been significant advancements in the definition of innovative minimal damage structures chasing the urgent requirements of more resilient societies against extreme seismic events. In this context, a type of seismic-resilient moment resisting frames (MRFs) is based on the use of Self-Centring Damage-Free (SCDF) devices in column bases and beam-to-column joints. However, when these devices are widespread across the whole structure, the details' complexity increases significantly with respect to conventional solutions, thus limiting their practical application. To overcome this drawback, current research works are focusing on the definition of optimum locations for SCDF devices such that their effectiveness is maximised. Within this context, the present study investigates optimum locations for a limited number of SCDF devices to be used within mid- and high-rise MRFs. An 8-storey structure is selected for case study purposes and nineteen configurations are investigated considering different positions of SCDF joints. Numerical models of the selected configurations are developed in OpenSees and Incremental Dynamic Analysis are performed. The seismic responses of the case-study structures equipped with different layouts of SCDF devices are evaluated and compared. Some considerations in terms of optimal distributions of SCDF devices are made with the aim of maximising the efficiency of the solution and the seismic performance of mid- and high-rise MRFs.

Keywords

Moment Resisting Steel Frames, Self-Centring, Damage-Free Column Bases, Damage-Free Beam-to-Column Connections, Structural Resilience

1 Introduction

Traditional seismic design methods, suggested by most current codes and guidelines and conventionally applied worldwide, are based on energy dissipation related to construction damage. These strategies imply large direct (*e.g.*, casualties, repair cost) and indirect (*e.g.*, downtime) losses. Additionally, due to the high seismic demand related to severe seismic events, structures might experience significant residual deformations, impairing the repairability. These situations strongly affect the overall resilience of communities subjected to extreme events, especially when the damaged structures include strategic facilities such as hospitals, fire stations, etc that must remain operational in the aftermath of a damaging earthquake. In this direction, nowadays Earthquake Engineering is facing an extraordinarily challenging era coping with the task of providing low-cost, thus more widely affordable, high-seismic-performance structures capable of sustaining a design level earthquake with limited socio-economical losses. Within this context, many recent research studies focused on the development of innovative seismic resilient structures chasing the objectives of minimising both seismic damage and repair time, hence allowing the definition of structures able to go back to the undamaged, fully functional condition in a short time [*e.g.*, 1, 2].

Focusing on steel Moment Resisting Frames (MRFs), the design strategy defined in modern codes [*e.g.*, 3, 4] is based on principles of "capacity design". As well known, the standardised design procedure results in over-strengthened columns and connections leading to structures characterised by weak beams and Column Bases (CBs), with strong joints. This approach, on one hand, allows reaching the safety requirements specified in the seismic codes, on the other hand, it implies high direct and indirect losses. In order to satisfy the compelling needs of cost-effectiveness and high-seismic performance, a wide range of low-damage solutions have been proposed for MRFs. Among others, in this type of structures, the conventional full-strength connections can be replaced by dissipative partial strength joints where yielding or Friction Devices (FDs) represent the weakest part of the connection. This approach allows a significant improvement in terms of reparability of the structure while not affecting its seismic performance. Many theoretical and experimental works, as well as practical applications, were carried out [*e.g.*,

1. University College London, London, UK.
2. University of Salerno, Salerno, Italy.

5, 6], including FDs in Beam-to-Column Joints (BCJs). Recently, within the European project FREEDAM [7], a new low-damage joint typology based on symmetric FDs has been proposed for the application in steel MRFs [8]. Although the use of beam-to-column connections equipped with FDs can be an efficient solution to protect the frame components from damage, it does not allow the control of the residual drifts. This issue has been tackled by several researchers by introducing elastic restoring forces able to regulate the self-centring capability of the structure through self-centring beam-to-column connections [*e.g.*, 9, 10]. Besides, it has been shown that protecting CBs from damage is an essential requirement for seismic-resilient structures. To this scope, several researchers proposed Self-Centring Damage-Free (SCDF) connections also in the CBs [*e.g.*, 11-14]. It is noteworthy that most of these studies [*e.g.*, 11, 14] have focused on the use of SCDF CBs within MRFs also equipped with SCDF BCJs demonstrating advantages in terms of both self-centring capabilities and damage-free behaviour. Nevertheless, a drawback of these solutions is the complexity of the structural details. In fact, if on the one hand the widespread use of SCDF devices is expected to produce a fully damage-free and self-centring response, on the other hand, it may represent a limit to the practical application, because of the increase of the realisation effort compared to conventional buildings. To overcome this limitation, current research studies are focusing on the investigation of optimum locations for SCDF devices such that their effectiveness is maximised. In this direction, Elettore et al. [15], while investigating a four-storey steel MRF, showed that the introduction of SCDF CBs results as an effective measure in limiting the residual drifts and protects the first storey columns from yielding without any detrimental effect on the peak values of the seismic demands. Further research studies have been carried out investigating the influence of the frame's layout on the self-centring capability of MRFs equipped with the SCDF CBs connections. In this context Elettore et al. [16] while performing a parametric analysis of nine case studies with a different number of storeys and bays, demonstrated that the use of SCDF systems localised only at the CBs is very effective in improving the self-centring capabilities of low-rise buildings, but their efficiency for mid- and high-rise buildings is significantly reduced.

In this context, the present work investigates the optimal placement of a limited number of SCDF devices applied in both CBs and BCJs, such that their effectiveness is maximised. For case study purposes a type of SCDF connection is considered, an 8-storey MRF structure is selected as a prototype building and nineteen different configurations are investigated. Finite element models are developed in Opensees [17] and non-linear time-history analyses are performed in an Incremental Dynamic Analysis fashion. The seismic performance of all the configurations is evaluated and compared. Some conclusions are drawn towards the identification of the optimal placement of a limited number of SCDF devices that maximise the effectiveness of the solution and the seismic performance of such MRFs.

2 Methodology

The SCDF CB and BCJs used in this study are based on the one proposed and experimentally investigated by Latour et al. [13]. A design procedure, able to satisfy and easily control: 1) the yielding of the first storey columns; 2) the self-centring capability; 3) the gap opening mechanism, is proposed and applied. Partial safety factors for the components and materials of the connection are assumed to satisfy the aforementioned conditions. An 8-storey 3-bays MRF case study frame is considered, and three reference frames are designed: 1) the MRF with conventional CBs and full-strength BCJs; 2) the equivalent MRF equipped with the SCDF CBs (CB); 3) the equivalent MRF equipped with SCDF connections in both CBs and all BCJs (CB-BCJALL). Sixteen additional frames (CB-BCJ) are successively investigated, considering SCDF CBs and different layouts of a limited number of SCDF BCJs. The aim is to elucidate the trends, delineating a strategy for the identification of the best compromise in terms of improved seismic response and reduced number of devices. State-of-the-art numerical models are developed in OpenSees [17] for all the frames. Non-linear static push-pull analyses are performed to monitor the local behaviour of the structure hence: 1) the formation of plastic hinges; 2) the elastic behaviour of the panel zones; 3) the designed behaviour of SCDF joints. Additionally, non-linear time-history analyses are performed in an Incremental Dynamic Analyses (IDA) [18] fashion to evaluate the seismic response of each configuration. IDAs are carried out on a set of 30 ground motion records to account for the influence of the uncertainty related to the earthquake input, *i.e.*, the record-to-record variability. The effects of model parameter uncertainty and epistemic uncertainty are less notable than the effects of record-to-record variability [19] and hence they are not considered in this study. Average spectral acceleration in the range of periods of the stiffest and more flexible structure is assumed as Intensity Measure (IM) and Peak and Residual interstorey drift are chosen as Engineering Demand Parameters (EDPs).

3 Self-Centring Damage-Free Joint

Figure 1 shows two schematic representations of the considered SCDF CB and SCDF BCJ which configurations are based on Latour et al. [13]. The proposed connection is a combination of FDs, which dissipate the seismic input energy, and a re-centring system composed of Post-Tensioned (PT) bars and disk springs, which control the self-centring behaviour of the connection.

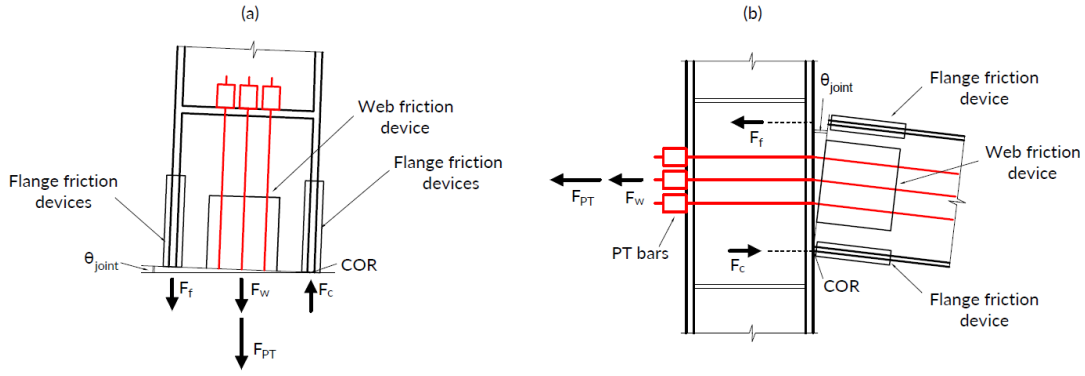

Figure 1 Schematic representation of the considered SCDF connection with the expected forces in the components during the gap-opening phase. (a) CB; (b) BCJ

Two slightly different structural configurations are used for CBs and BCJs. For CBs the first storey column is divided into two parts, a lower and an upper part, connected by the presence of plates bolted to the column's web and flanges. For BCJs plates are bolted to the beam's web and flanges. Friction pads are inserted between the element section and the plates. To allow the gap opening, a system of holes and slots is realised in the upper column section along the web and the flanges for CBs, and in the beam section along the web and the flanges for BCJs. During the gap opening the column and the beam sections rotate around their extremities while the steel plates remain fixed. Therefore, the FDs are realised slotting the column section (for CBs) and the beam section (for BCJs), adding cover plates, and including friction pads pre-stressed with high strength pre-loadable bolts on both web and flanges of columns (for CBs) and beams (for BCJs). The so obtained damper typology dissipates energy through the alternate slippage of surfaces in contact, on which a transversal force is applied by means of high strength bolts. The cyclic behaviour of web and flanges FDs is characterised by a rigid-plastic hysteretic model, which depends on the clamping force and the friction coefficient of the contact interfaces. A system of PT bars equipped with disk springs is included to ensure the self-centring behaviour of the connection. PT bars do not possess low enough stiffness and high enough resistance simultaneously, in order to allow the gap opening without engaging in the plastic range. Therefore, each PT bar is equipped with a set of disk springs to provide the ideal stiffness–resistance combination to the system. Disk springs are arranged into two different configurations which have different functions within the re-centring system. The disk springs in parallel control the yielding resistance of the re-centring system while the disk springs in series control the stiffness. PT bars are symmetrically located along the web's dept of the structural elements: columns for CBs and beam for BCJs.

3.1 Expected Forces in the components

The design of SCDF joints is based on the knowledge of the design forces developed in the connection during the gap-opening phase (Figure 1). The forces in the FDs are slippage forces related to the alternate slippage of surfaces in the web (F_w) and flanges (F_f). They can be calculated as follows:

$$\boldsymbol{F_w = F_{slip,w} = \mu \cdot n_s \cdot n_{bw} \cdot F_{p,w}} \quad (1)$$

$$\boldsymbol{F_f = F_{slip,f} = \mu \cdot n_s \cdot n_{bf} \cdot F_{p,f}} \quad (2)$$

where μ is the design value of the friction coefficient; n_s is the number of friction surfaces and is equal to 2; n_{bw} is the total number of bolts in the web; n_{bf} is the total number of bolts in the flanges; $F_{p,w}$ and $F_{p,f}$ are the design pretension forces on each bolt respectively on the web and the flanges, and they are orthogonal to the considered friction surfaces.

The forces in the re-centring system are those related to its re-centring capacity. F_{PT} simulate the axis behaviour of the whole system composed of PT bars and disk springs and it is defined as follows:

$$\boldsymbol{F_{PT} = F_{PT,0} + \Delta F_{PT}} \quad (3)$$

where $F_{PT,0}$ is the initial pretension force in the PT bars; ΔF_{PT} is the extra force occurring in the system during the gap opening phase.

$$\boldsymbol{F_{PT,0} = n_{PT} \cdot F_{p,PT}} \quad (4)$$

$$\boldsymbol{\Delta F_{PT} = K_{eq} \cdot \Delta l_{PT}} \quad (5)$$

where n_{PT} is the total number of PT bars; $F_{p,PT}$ is the design pretension forces on each PT bar; K_{eq} is the equivalent stiffness of the whole system composed by PT bars and disk springs; Δl_{PT} is the elongation of the PT bars considering their axis behaviour.

K_{eq} can be calculated as

$$\boldsymbol{K_{eq} = n_{PT} \cdot \frac{K_{PT} \cdot K_{DS}}{K_{PT} + K_{DS}}} \quad (6)$$

where K_{PT} is the stiffness of a single PT bar; and K_{DS} is the stiffness of a set of disk springs arranged both in series and in parallel. These partial stiffnesses can be evaluated as

$$\boldsymbol{K_{TB} = \frac{E_{PT} \cdot A_{s,res,PT}}{L_{PT}}} \quad (7)$$

$$\mathbf{K_{DS} = \frac{n_{par}}{n_{ser}} \cdot K_{DS1}} \quad (8)$$

where E_{PT} is the elastic modulus of the PT bars; $A_{s,res,PT}$ is the resistance area of a PT bar; L_{PT} is the length of the PT bars; n_{par} and n_{ser} are respectively the number of disk springs arranged in parallel and in series; K_{DS1} is the stiffness of one disk spring.

The elongation of the PT bars (Δl_{TB}), considering their axis behaviour, is assumed linearly proportional to the rotation of the joint. It is evaluated at the maximum target rotation (ϑ_{joint}) as follows:

$$\boldsymbol{\Delta l_{PT} = \theta_{joint} \cdot \left(\frac{h - t_f}{2}\right)} \quad (9)$$

where h and t_f are respectively the height and the flange's thickness of the cross-section of the structural element; ϑ_{joint} is the maxim target rotation of the SCDF joint and it is assumed equal to 40 mrad, which is the benchmark rotation established by AISC 341-16 [4] for Special MRFs.

3.2 Moment-rotation relationship

The behaviour of the connection is characterised by two phases. A closed phase and a gap-opening phase. The forces in the web and flanges FDs (F_w and F_f) are completely developed in the closed phase and their contribution remains constant during the gap opening. The pretension forces on the PT bars ($F_{p,PT}$) are an initial condition, while the extra forces in the re-centring system (ΔF_{PT}) occur just during the gap opening phase and linearly vary with the joint's rotation.

The contributions to be considered in order to define the moment-rotation behaviour of the connection are shown in Figure 2(a) and can be calculated, with respect to the centre of rotation, by using the following relations:

$$\boldsymbol{M_N = N_{Ed} \cdot \left(\frac{h - t_f}{2}\right)} \quad (10)$$

$$\boldsymbol{M_{PT,0} = F_{PT,0} \cdot \left(\frac{h - t_f}{2}\right)} \quad (11)$$

$$\boldsymbol{M_{FD} = M_{FD,w} + M_{FD,f} = F_w \cdot \left(\frac{h - t_f}{2}\right) + F_f \cdot (h - t_f)} \quad (12)$$

$$\boldsymbol{M_{PT,\theta} = \Delta F_{PT} \cdot \left(\frac{h - t_f}{2}\right) = K_{eq} \cdot \theta_{joint} \cdot \left(\frac{h - t_f}{2}\right)^2} \quad (13)$$

Therefore, the decompression moment (M_D) and the elastic resisting moment (M_E) of the connection can are defined using the following relations:

$$\boldsymbol{M_D = M_N + M_{PT,0}} \quad (14)$$

$$\boldsymbol{M_E = M_D + M_{FD} = M_N + M_{PT,0} + M_{FD}} \quad (15)$$

The moment-rotation behaviour of the SCDF joints can be represented by the flag-shape curve shown in Figure 2(b) It can be defined by four fundamental values of the moment: the maximum and the minimum moment at zero rotation (M_1, M_3), the maximum and the minimum moment at the target rotation ϑ_{joint} (M_3, M_4). They can be calculated as follow:

$$\boldsymbol{M_1 = M_E = M_N + M_{PT,0} + M_{FD}} \quad (16)$$

$$\boldsymbol{M_2 = M_1 + M_{PT,\vartheta}} \quad (17)$$

$$\boldsymbol{M_3 = M_2 - 2 \cdot M_{FD}} \quad (18)$$

$$\boldsymbol{M_4 = M_1 - 2 \cdot M_{FD}} \quad (19)$$

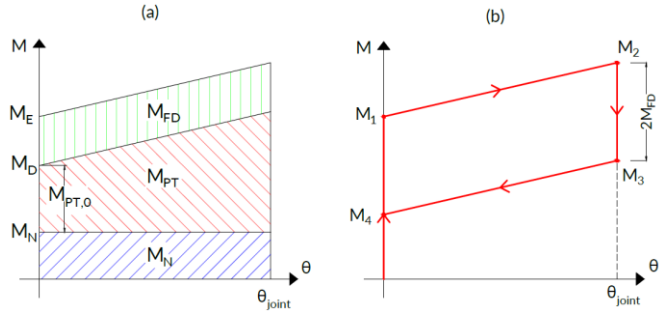

Figure 2: Moment-rotation behaviour of the SCDF joint. (a) Moment contributions: M_N, M_{PT}, M_{FD}; (b) Flag shape hysteretic behaviour

3.3 Design Procedure

The design procedure requires as input parameters: i) the cross-section properties of the structural element; ii) the maximum and minimum axial force ($N_{Ed,min}$, $N_{Ed,max}$); iii) the bending moment (M_{Ed}) in the structural element due to the seismic combination for the Design Based Earthquake (DBE); iv) the yielding moment of the structural element (M_y). Two partial safety factors are applied in order to consider the random variability of the friction coefficient (γ_μ) and the pretension forces (γ_{PT}). Based on previous tests on friction materials [20] γ_μ is assumed equal to 1.39 while γ_{PT} is assumed equal to 1.2 according to EN 1090-2 [21]. Therefore, two safety factors are defined, one for FDs (α_{FD}) and on for PT (α_{PT}) bars, as follows:

$$\boldsymbol{\alpha_{FD} = \gamma_\mu \cdot \gamma_{PT} = 1.67} \quad (20)$$

$$\boldsymbol{\alpha_{PT} = \gamma_{PT} = 1.2} \quad (21)$$

The objective of the design procedure is to satisfy at the same time three main conditions: 1) no damage of the structural element, 2) self-centring behaviour of the structure, 3) occurrence of the gap opening after the seismic design situation at DBE. The aforementioned conditions can be summarised in the following system of inequalities:

$$\begin{cases} \boldsymbol{M_2 < M_y} \\ \boldsymbol{M_4 > 0 \rightarrow M_D > M_{FD}} \\ \boldsymbol{M_1 > M_{Ed}} \end{cases} \quad (22)$$

In order to ensure a higher level of safety the three conditions are considered with the unfavourable combination of axial loads and safety factors as follows 1) for the no damage condition ($N_{Ed,max}$, α_{FD}, α_{PT}), 2) for the self-centring condition ($N_{Ed,min}$, α_{FD}), 3) for the gap opening condition ($N_{Ed,min}$, no coefficients). A simple rearrangement of Equation (22) leads to:

$$\begin{cases} \boldsymbol{\alpha_{PT} \cdot M_{PT,0} + \alpha_{FD} \cdot M_{FD} + M_{PT,\vartheta} < M_y - M_{N_{Ed,max}}} \\ \boldsymbol{M_{PT,0} - \alpha_{FD} \cdot M_{FD} > -M_{N_{Ed,min}}} \\ \boldsymbol{M_{PT,0} + M_{FD} > M_{Ed} - M_{N_{Ed,min}}} \end{cases} \quad (23)$$

Therefore, the design procedure consists of solving a system of three inequalities with three unknown variables ($M_{PT,0}$, M_{FD}, $M_{PT,\vartheta}$).

Assuming that the moment due to slippage forces in the FDs (M_{FD}) is equally distributed among the FDs of web and flanges, the contributions of moment $M_{FD,w}$ and $M_{FD,f}$ can be evaluated as:

$$\boldsymbol{M_{FD,w} = M_{FD,f} = \frac{M_{FD}}{2}} \quad (24)$$

Deriving $M_{PT,0}$, $M_{FD,w}$, $M_{FD,f}$ and $M_{PT,\vartheta}$ from Equations (23) and (24), it is possible to calculate $F_{PT,0}$, F_w, F_f and K_{eq} by inverting Equations (11),(12) and (13). Therefore the number of bolts along the web and the flanges (n_{bw}, n_{bf}) and the number of PT bars (n_{PT}) can be evaluated by choosing the diameter and the class of bolts and PT bars, inverting Equations (1), (2) and (4) and ensuring that the pretension force in each bolt ($F_{p,w}$ and $F_{p,f}$) and Pt bar ($F_{p,PT}$) is smaller than the maximum pretension force ($F_{p,max}$) defined as:

$$\boldsymbol{F_{p,max} = \frac{0{,}7 \cdot A_{s,res} \cdot f_{ub}}{\gamma_{M7}}} \quad (25)$$

where $A_{s,res}$ is the resistance area of the bolt or PT bar; f_{ub} is the ultimate strength of the employed steel; γ_{M7} is the coefficient for the pretension force which is 1.1 for bolts and 1 for PT bars according to Eurocode 8 [3].

Additionally, the number of disk springs in parallel and can be evaluated by firstly choosing the type of the disk spring and the length of PT bars. Thus, for disk springs in parallel (n_{par}), the stiffness of a single PT bar needs to be calculated by Equation (7) and the following relation has to be applied in order to avoid the yielding of the PT bars:

$$\boldsymbol{F_{y,DS} \geq F_{y,TB} \rightarrow n_{par} \geq \frac{A_{s,res,PT} \cdot f_y}{F_{y,DS1}}} \quad (26)$$

where $A_{s,res,PT}$ is the resistance area of a PT bar; f_y is the yielding strength of the steel used for the PT bars; $F_{y,DS1}$ is the yielding strength of one disk spring.

The number of disk springs in series (n_{ser}) can be evaluated by substituting Equation (8) in (6) and inverting it.

4 Case study Structures

The investigated case study is an 8-storey steel building with an interstorey height of 3.50 m for the first level and 3.20 m for the others. The plan layout consists of 5 bays in the x-direction and 3 bays in the y-direction with a constant span of 6.0 m. Seismic resistant perimeter MRFs are located in the x-direction and y-direction while the interior part is composed of gravity frames (with 'pinned' BCJs and 'pinned' CBs).

The present study focuses on the assessment of the seismic resisting frames in the x-direction. The plan and elevation view of the case study is reported in Figure 3. In order to define the optimal location for SCDF joints within the structures nineteen configurations frames are investigated: three reference configurations (MRF, CB and BCJALL) and sixteen additional configurations (CB-BCJ) with SCDF CBs and different positions of a limited number of SCDF BCJs. In Figure 4 a summary of the investigated configurations is reported.

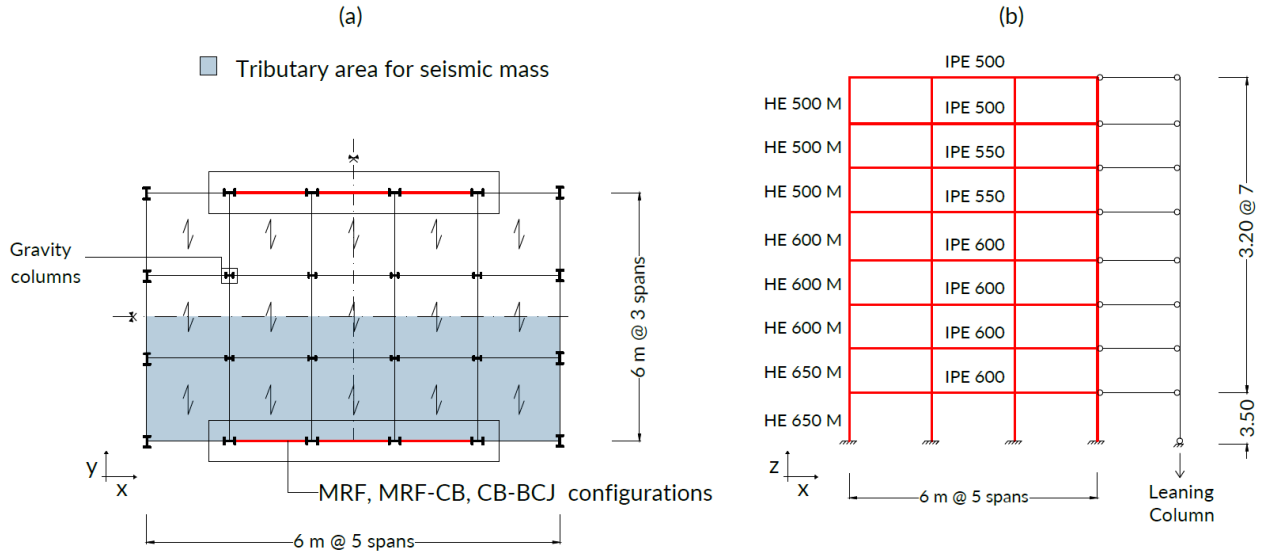

Figure 3 (a) Plan view and (b) Elevation view of the case study frame

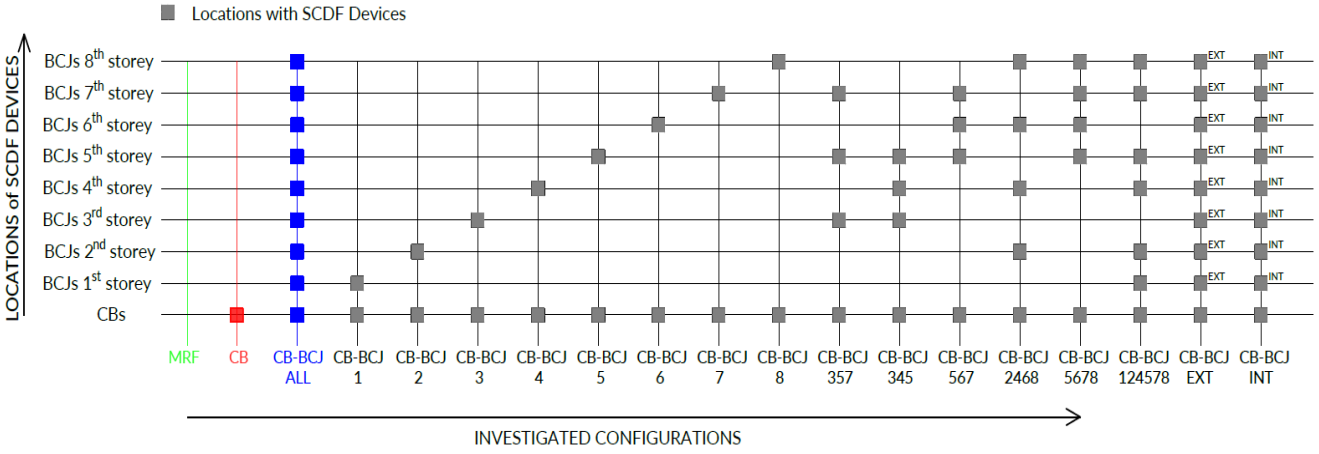

Figure 4 Summary of the investigated configurations

4.1 Design of the Moment Resisting Frame

The MRF is designed according to Eurocode 8 [3] requirements. Two steel grades are used for dissipative and non-dissipative zones. Hence the steel yield strength used is 355 MPa for the columns and 275 MPa for the beams. The DBE (*i.e.*, probability of exceedance of 10% in 50 years) is defined considering the Type 1 elastic response spectrum with a peak ground acceleration of 0.35g and a soil type C. The Maximum Credible Earthquake (*i.e.*, MCE, probability of exceedance of 2% in 50 years) is assumed to have an intensity equal to 150% the DBE. Since the structure represents an ordinary building, it belongs to important class II and an importance factor equal to 1 is considered. The building is characterised by plan and elevation regularity. The behaviour factor is evaluated according to the provisions of the Eurocode 8 [3] for MRFs in DCH, hence assumed as q=6.5. The structure has non-structural elements fixed in a way so as not to interfere with structural deformations. Therefore, the interstorey drift limit for the Frequently Occurred Earthquake requirements (*i.e.*, FOE, probability of exceedance of 10% in 10 years) is assumed as 1% accordingly to Eurocode 8 recommendations [3]. The most stringent requirement for MRF is the limitation of the interstory drift at FOE which governs the design procedure. Beams' and columns' profiles deriving from the design of the MRF are reported in Figure 3 (b). Additionally, in order to promote the occurrence of plastic hinges only at the ends of the beams, the panel zones are stiffened with doubler plates with a thickness equivalent to the column's web. The mass of each storey is evaluated based on the seismic combination of the Eurocode 8 [3].considering the tributary area for seismic mass and adding the self-weight of the deigned structural elements. The internal gravity frame is designed to resist only the gravity loads.

4.2 Design of the CB connection

The SCDF CBs is designed following the procedure described in Section 3.3. It is worth reminding that the cross-section profile of the first storey column is an HE 650 M. Two different configurations of the CBs are defined: one for the external columns (CB-EXT), which are subjected to the high variability of the axial force during the seismic event, and one for the internal columns (CB-INT). The design actions are derived based on the linear static analysis (lateral force method) of the equivalent frame with full-strength CB connections (MRF). The maximum and minimum axial force ($N_{Ed,min}$, $N_{Ed,max}$), and the bending moment (M_{Ed}) of the external and internal columns are taken from the seismic combination of the Eurocode 8 [3] for DBE, considering the proper location of the CBs. In order to avoid the occurrence of plastic hinges in the first storey columns, their lower part is reinforced through steel plates bolted to the flanges and characterised by a thickness of 30 mm. Therefore the yielding moment of the column (M_y), to be considered in the design procedure, takes into account the stiffened section. The design input information for external and internal columns are reported in Table 1

where – stands for tension and + for compression. The friction coefficient (μ) is assumed equal to 0.53 which is the recommended dynamic friction coefficient value for material M4 [22]. The following properties are chosen for the components of the CB connection: HV M30 10.9 class bolts for web and flanges FDs, HV M39 10.9 class PT bars with a length of 1.7 m, disk springs with a yielding strength ($F_{y,DS1}$) equal to 250 kN and a stiffness (K_{DS1}) of 96 kN/mm. The results of the design procedure obtained for external and internal columns are reported in Table 2.

Table 1 Design input for CBs

CB	Section Profile	$N_{Ed,min}$ [kN]	$N_{Ed,max}$ [kN]	M_{Ed} [kN·m]	M_y [kN·m]
EXT	HE 650 M	-1556	+2749	2025	4872
INT	HE 650 M	+855	+863	2138	4872

Table 2 Design results for CBs

CB	n_{bw} [-]	$F_{p,w}$ [kN]	n_{bf} [-]	$F_{p,f}$ [kN]	n_{PT} [-]	$F_{p,PT}$ [kN]	n_{par} [-]	n_{ser} [-]	K_{eq} [kN/mm]
EXT	4	282	2	282	10	562	4	20	161.6
INT	4	300	2	300	6	568	4	15	126.8

4.3 Design of the BCJ

The SCDF BCJs are designed following the procedure described in Section 3.3. It is worth reminding that the cross-section profile of the beams are: IPE 600 for 1st,2nd,3rd and 4th storey, IPE 550 for 5th and 6th storey, and IPE 500 for 7th and 8th storey. In this case, 6 different configurations of SCDF joints are defined: one internal (BCJ-INT) and one external (BCJ-EXT) for each selected cross-section. The design procedure is the same followed for CBs with a few main differences. Beams are not subjected to axial force therefore, the maximum and minimum axial forces ($N_{Ed,min}$, $N_{Ed,max}$) are equal to zero. The yielding moment of the beam (M_y), to be considered in the design procedure is the nominal one, since beams are not reinforced. The design input information for the three cross-sections, external and internal, are reported in Table 3.

Table 3 Design input for BCJs

BCJ Storey	Section Profile	N_{Ed} [kN]	M_{Ed} [kN·m]	M_y [kN·m]
1-4	IPE 600	0	455	810
5, 6	IPE 550 M	0	331	640
7, 8	IPE 500	0	188	508

Table 4 Design results for BCJs

BCJ Storey	n_{bw} [-]	$F_{p,w}$ [kN]	n_{bf} [-]	$F_{p,f}$ [kN]	n_{PT} [-]	$F_{p,PT}$ [kN]	n_{par} [-]	n_{ser} [-]	K_{eq} [kN/mm]
1-4 (EXT)	4	73	2	73	4	259	3	23	440.3
1-4 (INT)	4	73	2	73	4	259	3	49	220.2
5,6 (EXT)	4	59	2	59	4	212	3	20	506.4
5,6 (INT)	4	59	2	59	4	259	3	43	253.2
7,8 (EXT)	4	42	2	42	4	150	3	20	512.3
7,8 (INT)	4	42	2	42	4	259	3	42	256.1

K_{eq} is calculated differently for the internal and external configurations. For BCJ-EXT K_{eq} can be simply obtained by inverting Equation (13) as for CBs. For BCJ-INT the elongation of the PT bars considering its axis behaviour is no longer proportional to the rotation of the joint, since the PT bars are uninterrupted along the joint. Therefore, the elongation (Δl_{PT}) is proportional to two times the maximum target rotation of the joint ($2 \cdot \vartheta_{joint}$). Hence, for BCJ-INT, the K_{eq} can be calculated by inverting Equation (13) considering a doubled elongation of the PT bars. The friction coefficient (μ) is assumed as for CBs. The properties chosen for the components of the BCJ are the same as the CBs except for PT bars which are HV M36 10.9. The results of the design procedure obtained for the three cross-sections external and internal joints are reported in Table 4.

5 Finite Element Modelling

5.1 Frame modelling

A two-dimensional non-linear Finite Element (FE) model of the MRF is developed in OpenSees [17]. The 'Steel01' material [17] for 355 MPa yield strength and 275 MPa yield strength and 0.2% post-yield stiffness ratio, is employed for columns and beams, respectively. Beams are modelled with a lumped plasticity approach with an elastic internal part ('element elasticBeamColumn' [17]) and non-linear rotational springs ('element zeroLength' [17]) at beams' ends in order to model the plastic hinges. The rotational springs are defined with a bilinear hysteretic moment-rotation behaviour ('uniaxialMaterial Bilin' [17]) based on the modified Ibarra-Krawinkler deterioration model [23] implemented as suggested by Lignos and Krawinkler [24]. Columns are modelled as non-linear elements with distributed plasticity ('element nonlinearBeamColumn' [17]). The panel zones are modelled following the Scissor model [25]. The rigid slab behaviour is modelled by imposing the same horizontal displacements to the nodes belonging to the same storey ('equalDOF' [17]). Geometric nonlinearities are considered in the elements of the MRF ('geomTransf PDelta' [17]). Additionally, in order to consider the P-Δ effects related to the displacements and the axial forces of the gravity frame a leaning column is included in the structural model [26], as shown in Figure 3 (b). Distributed and concentrated loads are applied on beams and columns and masses are concentrated at the beam-column connections. Damping sources other than the hysteretic energy dissipation are modelled through the Rayleigh damping matrix. The values of the mass-related and stiffness-related damping coefficients are evaluated for a damping factor of 3% considering the first and the second vibration modes.

5.2 CB modelling

The CB connection is implemented following the modelling strategy proposed by Elettore et al. [*i.e.*, 15, 16]. The model of the CB has to be able to capture the variability of the axial force occurring in the column during the seismic event; therefore, each component needs to be modelled in detail. An advanced two-dimensional non-linear FE model of the CB is developed in OpenSees [17] as reported in Figure 5. The rocking interface is modelled with 8 horizontal rigid elements characterised by a very high flexural stiffness ('element elasticBeamColumn' [17]). The web and flanges FDs are modelled with 4 bilinear translational springs ('element zeroLength' [17]) placed in parallel, 2 internal for web FDs and 2 external for flanges FDs. They are defined by the 'Steel01' material [17] considering a very high initial stiffness and a very low post-elastic stiffness in order to model the rigid plastic behaviour, a yield strength equal to the slippage force in web and flanges FDs (F_w or F_f) obtained from the design procedure. The rocking behaviour is modelled with 4 translational springs ('element zeroLength' [17]) placed in parallel. They are defined by the 'Compression-no-tension (ENT)' material [17] and they exhibit an elastic compression-no tension force-displacement behaviour. The self-centring system composed of PT bars and disk springs is modelled by a single central translational spring ('element zeroLength' [17]). It is defined by the 'Steel01' material [17] considering: an initial elastic tangent equal to the equivalent stiffness of the self-centring system (K_{eq}); a yield strength defined as the minimum between $F_{y,DS}$ and $F_{y,TB}$, multiplied by n_{PT}; a post-yield stiffness

ratio of 1%. The initial pre-tensioning force ($F_{PT,0}$) is modelled by imposing an initial strain using the 'Initial strain material' [17] combined with the material 'Steel01' [17].

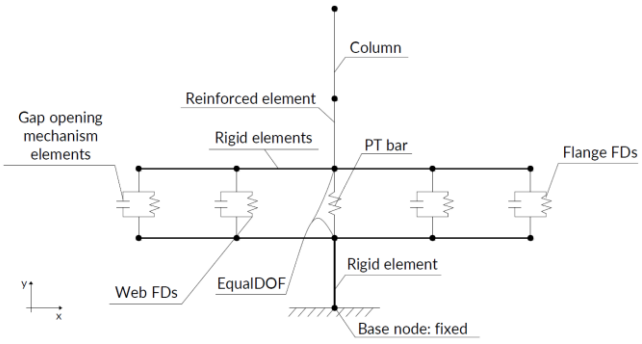

Figure 5 Two dimensional Opensees model of CB connection

5.3 BCJs modelling

Conversely to the CB's model, the BCJ's model does not need detailed modelling of each component since in the beams the axial force is equal to zero. Therefore, in order to relieve the computational complexity of the model, BCJs are implemented following a simplified modelling strategy similar to the one used to model the plastic hinges at the ends of the beams. BCJs are modelled as non-linear rotational springs ('element zeroLength' [17]) allocated at the ends of beams' replacing the plastic hinges. The rotational springs are defined with the design flag-shape moment-rotation behaviour ('uniaxialMaterial SelfCentering' [17]) considering: a very high initial stiffness; no slippage and no bearing.

6 Performance-Based Assessment

6.1 Push-pull Analysis

Non-linear static push-pull analyses are performed for the nineteen case study frames. The analyses are performed up to a roof displacement equal to 0.4 m which represents the displacement of the inelastic system at DBE. The relation between the roof displacement and the total base shear force, considering the contribution of the leaning column is shown in Figure 6(a) for the three reference configurations (MRF, CB, CB+BCJALL). The CB+BCJALL configuration is completely self-centring, showing the classical flag-shape behaviour while the MRF and CB are very closed to each other. This result is coherent with previous outcomes [16] according to which the effectiveness of SCDF CB connections decreases for mid- and high-rise buildings. The push-pull curves of the other configurations are between the CB curve and CB+BCJALL curve.

6.2 Incremental Dynamic Analysis

The nineteen configurations are characterised by slightly different vibration periods due to the different stiffness of the connections. However, all the case study frames have a fundamental period between 1.25 and 1.29 s. Therefore, it is useful to define T_{1m} which represents the mean fundamental period equal to 1.27s. Incremental Dynamic Analyses (IDA) [18] have been carried out to investigate the seismic performances of the nineteen case study frames. A suite of 30 ground motion records is selected from the SIMBAD Database using REXEL [27] accounting for the record-to-record variability. The same set of ground motions is selected for all case study frames with the following parameters: moment magnitude (M_w) ranging from 6 to 7, epicentral distance $R \leq 30\ km$ and spectrum-compatibility in the range of periods between $0.2T_{1m}$ and $2T_{1m}$. The mean elastic spectrum of the records is kept between 75% and 130% of the corresponding Eurocode 8 [3] based elastic response spectrum considered for the design. It is worth mentioning that a large number of zero acceleration points (*i.e.*, 40 s) have been added at the end of each record to allow the free vibrations to stop and correctly capture the residual deformations. In order to allow the comparison of the IDA's outcomes for the different configurations, the average spectral acceleration (*avgSa*), considering the range of periods from the stiffer to the most flexible structure, has been considered as IM. (*avgSa*) is equal to 0.6g and 0.9g respectively for the DBE and MCE which represent the two seismic intensities of interest. The IDA is performed by scaling the ground motion records to increasing IM values with a constant step of 0.1g up to 1.0g. Global and storey-level EDPs are monitored to investigate the effectiveness and optimal distributions of the proposed SCDF joints. Peak and residual interstorey drifts (ϑ_{peak}, ϑ_{res}) are considered story-level EDPs, while the maximum values of these quantities among all the storeys are used as global EDPs. In this context, the residual interstorey drift limit ($\vartheta_{res,lim}$) is assumed equal to 0.5% which, for building frames, is conventionally associated with building reparability [28].

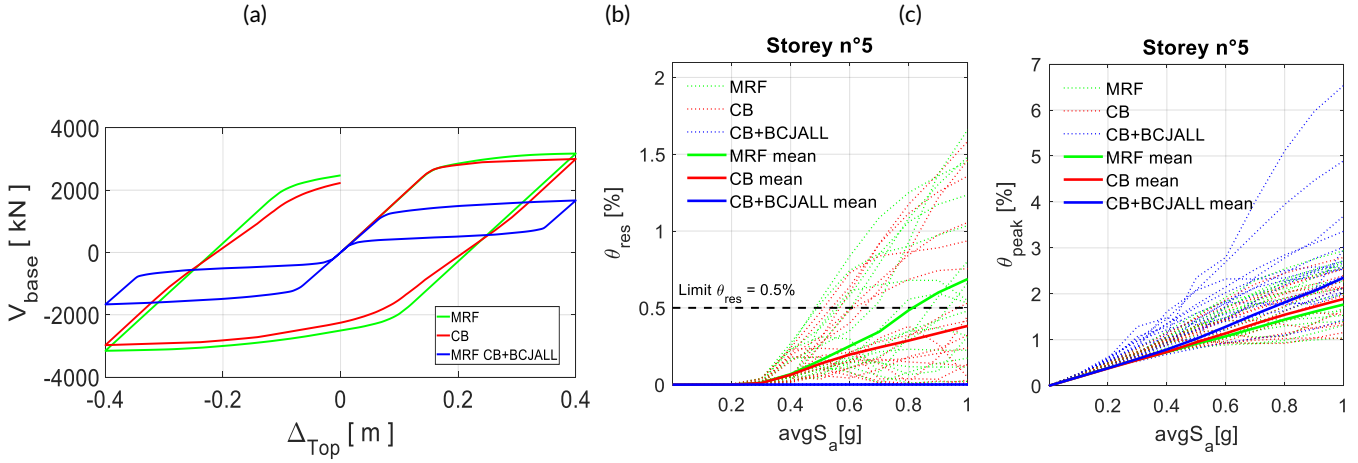

Figure 6 Results for (MRF, CB, CB+BCJALL): (a) Push-pull curve; IDA Results: (b) Residual interstorey drifts for storey n°5, (c) Peak interstorey drifts for storey n°5

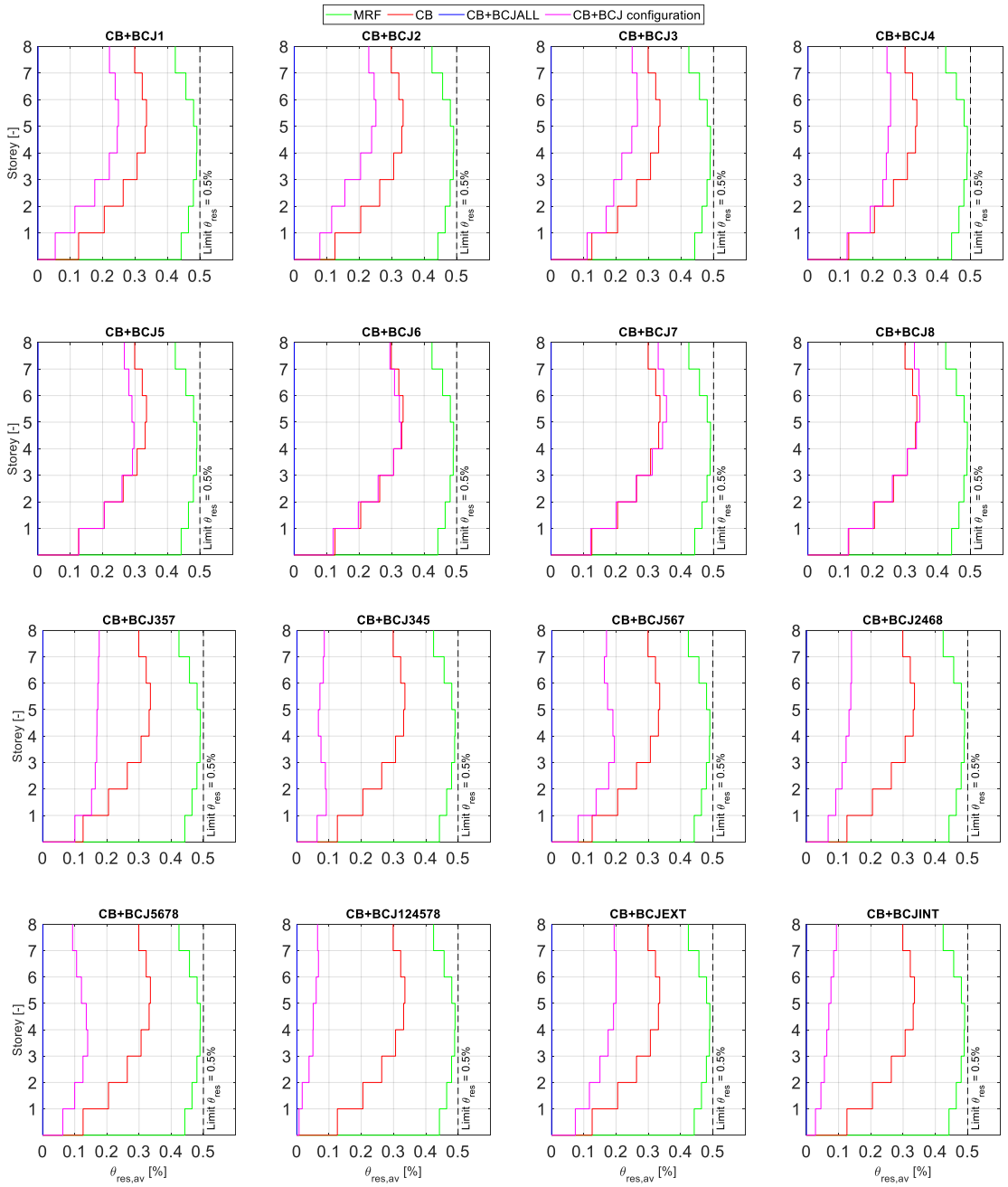

Figure 7 IDA Results: height-wise average residual interstorey drifts ($\theta_{res,av}$) at MCE. Comparison, between each configuration and the three reference configurations

The first interesting comparison can be done between the three reference configurations: MRF, CB and CB+BCJALL. Figure 6(b) and (c) illustrate the results of IDA in terms of ϑ_{res} and ϑ_{peak}, respectively. For the three aforementioned configurations, the results from each ground motion record and the mean values are reported. The samples of the demand (ϑ_{peak}, ϑ_{res}) vs the IM (*avgSa*) are shown just for storeys n° 5, but the results of the other storeys show a consistent trend in agreement with it. Based on Figure 6(b) and (c) the following considerations are made.

- In CB and CB+BCJALL there is a reduction of ϑ_{res} with respect to the MRF.
- In CB+BCJALL the structure results completely self-centred with ϑ_{res} equal to zero for all IMs.
- CB and CB-BCJALL the ϑ_{peak} of the structure are higher with respect to the MRF configuration.

In order to provide information about the trends of the monitored EDPs at all the storeys, their height-wise distribution is analysed. Figure 7 reports the average values of residual interstorey drifts ($\vartheta_{res,av}$) at MCE for all the storeys. For each configuration, the comparison with the three reference configurations is shown. From Figure 7, the following considerations are made.

- All the nineteen configurations have $\vartheta_{res,av}$ lower than the $\vartheta_{res,lim}$
- The CB+BCJ configurations with one level of SCDF BCJs (*e.g.*, CB+BCJ1, CB+BCJ2, *etc*) show that the effectiveness of the introduction of SCDFJs at only one storey-level decrease for higher storey-level. For example, in CB+BCJ6, CB+BCJ7 and CB+BCJ8 it results that the $\vartheta_{res,av}$ are equal or even higher than the ones of CB configuration.
- The configurations with more than one level of SCDF BCJs (*e.g.*, CB+BCJ357, CB+BCJEXT, *etc*) have a better response with respect to the configurations with one level of SCDF BCJs.
- Comparing the CB+BCJEXT and the CB+BCJINT configurations, it results that the second has smaller values of

$\vartheta_{res,av}$ since it includes a doubled number of SCDFJs.

- Focusing on the configurations with more than one level of SCDF BCJs it can be observed that a higher number of SCDFJs do not always lead to a better behaviour of the structure in terms of $\vartheta_{res,av}$. For example, CB+BCJ345 leads to smaller $\vartheta_{res,av}$ with respect to CB+BCJ2468 or CB+BCJ5678. This means that the position of the SCDFJs deeply influences the response of the structure.
- Configurations where SCDF BCJs are placed at adjacent storey-levels show a better performance in terms of $\vartheta_{res,av}$ with respect to the configurations where SCDF BCJs are placed at alternated storey-levels. (*e.g.*, CB+BCJ345 has lower $\vartheta_{res,av}$ with respect to CB+BCJ357).

Figure 8 shows global EDPs obtained as the maximum values of residual and peak interstorey drifts among all the storeys of each configuration ($\vartheta_{res,max}$ and $\vartheta_{peak,max}$). From Figure 8, the following considerations are made.

- For $\vartheta_{res,max}$ there is a high variability of the results among the configurations, while for $\vartheta_{peak,max}$ the values are very closed to each other.
- Accordingly, to the results shown in Figure 6(b) and (c) a minimum in terms of $\vartheta_{res,max}$ and a maximum in term of $\vartheta_{peak,max}$ can be observed for the CB+BCJALL configuration.
- There is not a correspondence between $\vartheta_{res,max}$ and $\vartheta_{peak,max}$, therefore many configurations with an optimal behaviour in terms of $\vartheta_{res,max}$ lead, at the same time, to hight $\vartheta_{peak,max}$. For example, the configuration which is the best in terms of $\vartheta_{res,max}$ at DBE is not the best for $\vartheta_{res,max}$ at DBE.
- There is not a clear correspondence between the results based on DBE and MCE; for example, the configuration that leads to a minimum $\vartheta_{res,max}$ at DBE is not the same that has the minimum $\vartheta_{res,max}$ at MCE.

7 Conclusions

The present study investigates optimum layouts of SCDF devices to be used within mid- and high-rise steel MRFs in order to maximise their effectiveness on the seismic performance of this type of structures. The SCDF connection used is based on the one proposed and experimentally tested by Latour et al. [13] and a design procedure has been defined in order to ensure the damage-free behaviour of the structural element (columns for CBs and beams for BCJs), the self-centring capability of the joint, and an adequate energy dissipation capacity. An 8-storey case study frame has been considered and several configurations have been investigated with different positions of the SCDF joints. Non-linear finite element models are developed in OpenSees [17] for all the configurations. Non-linear static push-pull analyses are carried on in order to monitor the local behaviour of the structure. Additionally, IDA analyses are performed considering *avgSa* as IM and ϑ_{res} and ϑ_{peak} as EDPs. The seismic responses of the different structural configurations are evaluated and compared, and the following conclusions are drawn.

- The inclusion of SCDFJs CBs and BCJs within a mid- and high-rise steel MRF results as an effective solution in protecting the structural elements from damage, avoiding the formation of plastic hinges at the bottom of the first storey columns and at the beam's ends.
- SCDFJs placed at hight storey-level do not have an effective influence on the seismic performance of the structure.
- In order to maximise the seismic response of the structure more than one level of SCDFJs has to be included.
- Both the number and the position of the SCDFJs deeply influence the seismic response of the structure.
- SCDFJs are an effective strategy in reducing the residual interstorey drift but lead to higher peak interstorey drifts.
- The optimal configuration has to be a good compromise between the response in terms of peak and residual interstorey drifts and it has to be a robust solution valid for every level of seismic input.

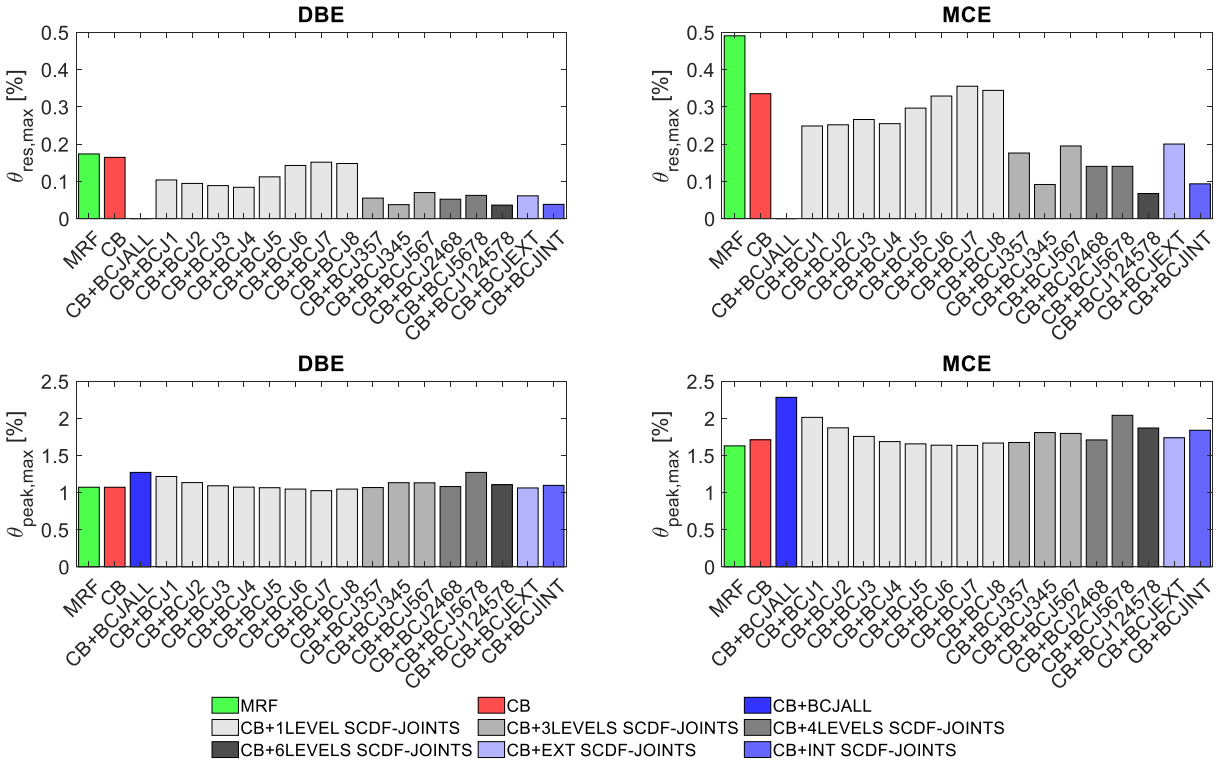

Figure 8 IDA Results: global EDPs in terms of maximum residual and peak interstorey drifts ($\vartheta_{res,max}$ and $\vartheta_{peak,max}$) for each configuration for both DBE and MCE

References

[1] MacRae, G.; Clifton, C.; Bruneau, M. (2018) *New Zealand Research Applications of, and Developments in, Low Damage Technology for Steel Structures*. Key Engineering Materials, 763, 3-10.

[2] Pampanin, S. (2012) *Reality-check and renewed challenges in Earthquake Engineering: implementing low-damage systems – from theory to practice*. Bulletin of the New Zealand Society for Earthquake Engineering, 45(4), 137-160

[3] EN 1998-1. *Eurocode 8: Design of structures for earthquake resistance – Part 1: General rules, seismic actions and rules for buildings*. (2004) European Committee for Standardization, Brussels.

[4] ANSI/AISC 341-16. *Seismic provisions for structural steel buildings, American Institute of Steel Construction*. (2016) Chicago, USA.

[5] Nastri, E.; D'Aniello, M.; Zimbru, M.; Streppone, S.; Landolfo, R.; Montuori, R.; Piluso, V. (2019). *Seismic response of steel Moment Resisting Frames equipped with friction beam-to-column joints*. Soil Dynamics and Earthquake Engineering, 119, 144-157.

[6] Latour, M.; D'Aniello, M.; Zimbru, M.; Rizzano, G.; Piluso, V.; Landolfo, R. (2018). *Removable friction dampers for low-damage steel beam-to-column joints*. Soil Dynamics and Earthquake Engineering, 115, 66-81.

[7] *FREEDAM: FREE from DAMage steel connections*. (2015-2018) Final report, Fund for Coal and Steel Grant Agreement No. RFSR-CT-2015-00022.

[8] Latour M.; Piluso, V.; Rizzano, G. (2018) *Experimental analysis of BCJs equipped with sprayed aluminium friction dampers.* Journal of Structural Engineering, 146, 33–48.

[9] Ricles, J.; Sause, R.; Garlock, M.; Zhao, C. (2001) *Posttensioned Seismic-Resistant Connections for Steel Frames*. Journal of Structural Engineering (ASCE), 127(2), 113–121.

[10] Dimopoulos, A.I.; Karavasilis, T.L.; Vasdravellis, G.; Uy, B. (2013) *Seismic design, modelling and assessment of self-centering steel frames using post-tensioned connections with web hourglass shape pins*. Bulletin of Earthquake Engineering, 11(5), 1797-1816.

[11] Freddi, F.; Dimopoulos, C. A.; & Karavasilis, T. L. (2017) *Rocking damage-free steel CB with friction devices: design procedure and numerical evaluation.* Earthquake Engineering & Structural Dynamics, 46(14), 2281-2300.

[12] Freddi, F.; Dimopoulos, C. A.; Karavasilis, T. L. (2020) *Experimental Evaluation of a Rocking Damage-Free Steel CB with Friction Devices*. Journal of Structural Engineering, 146(10), 04020217:1-20.

[13] Latour, M.; Rizzano, G.; Santiago, A.; da Silva, L. S. (2019) *Experimental response of a low-yielding, self-centering, rocking CB joint with friction dampers.* Soil Dynamics and Earthquake Engineering, 116, 580-592.

[14] Kamperidis, V. C.; Karavasilis, T. L.; Vasdravellis, G. (2018) *Self-centering steel CB with metallic energy dissipation devices.* Journal of Constructional Steel Research, 149, 14-30.

[15] Elettore, E.; Freddi F.; Latour M.; Rizzano G. (2021) *Design and analysis of a seismic resilient steel moment-resisting frame equipped with damage-free self-centring CBs*. Journal of Constructional Steel Research, 179: 106543.

[16] Elettore, E.; Lettieri, A.; Freddi, F.; Latour, M., & Rizzano, G. (2021, August) *Performance-based assessment of seismic-resilient steel moment resisting frames equipped with innovative column base connections.* In Structures (Vol. 32, pp. 1646-1664). Elsevier.

[17] Mazzoni, S.; McKenna, F.; Scott, M.H.; Fenves, G.L. (2009) *OpenSEES: Open System for earthquake engineering simulation*. Pacific Earthquake Engineering Research Centre (PEER), University of California, Berkley, California. Available at http://opensees.berkeley.edu.

[18] Vamvatsikos, D.; Cornell, C. A. (2002). *Incremental dynamic analysis.* Earthquake engineering & structural dynamics. 31(3), 491-514.

[19] Kwon, O. S.; Elnashai, A. (2006). *The effect of material and ground motion uncertainty on the seismic vulnerability curves of RC structure*. Engineering structures, 28(2), 289-303.

[20] Francavilla, A. B.; Latour, M.; Piluso, V.; & Rizzano, G. (2020). *Design criteria for beam-to-column connections equipped with friction devices.* Journal of Constructional Steel Research, 172, 106240.

[21] EN 1090-2. (2008) *Execution of Steel Structure and Aluminium Structure: Technical Requirements for Steel Structures.*

[22] Latour, M.; Piluso, V.; Rizzano, G. (2015). *Free from damage BCJs: Testing and design of DST connections with friction pads.* Engineering Structures, 85, 219-233.

[23] Ibarra, L. F.; Medina, R. A.; Krawinkler, H. (2005). *Hysteretic models that incorporate strength and stiffness deterioration.* Earthquake engineering & structural dynamics, *34*(12), 1489-1511.

[24] Lignos, D. G.; & Krawinkler, H. (2011). *Deterioration modeling of steel components in support of collapse prediction of steel moment frames under earthquake loading*. Journal of Structural Engineering, 137(11), 1291-1302.

[25] Charney, F. A.; Downs, W. M. (2004). *Modeling procedures for panel zone deformations in moment resisting frames.* Connections in Steel Structures. ESSC/AISC Workshop, Amsterdam.

[26] El Jisr, H.; Elkady, A.; Lignos, D. G. (2020). *Hysteretic behaviour of moment-resisting frames considering slab restraint and framing action*. Journal of Structural Engineering, 146(8), 04020145.

[27] Iervolino, I.; Galasso, C.; Cosenza, E. (2010). *REXEL: computer aided record selection for code-based seismic structural analysis.* Bulletin of Earthquake Engineering, 8(2), 339-362.

[28] McCormick, J.; Aburano, H.; Ikenaga, M.; Nakashima, M. (2008, October). *Permissible residual deformation levels for building structures considering both safety and human elements.* In Proceedings of the 14th world conference on earthquake engineering (pp. 12-17).